Published in final edited form as:
Anal Chem. 2008 August 1; 80(15): 6045–6050. doi:10.1021/ac800843v.

Fabrication of Microfluidic Reactors and Mixing Studies for Luciferase Detection

Qian Mei[†,‖], **Zheng Xia**[†], **Feng Xu**[‡,§], **Steven A. Soper**[*,‡], and **Z. Hugh Fan**[*,†]
Department of Mechanical and Aerospace Engineering, University of Florida, P.O. Box 116250, Gainesville, Florida 32611, Department of Chemistry, Louisiana State University, Baton Rouge, Louisiana 70803, and Department of Biomedical Engineering, University of Florida, P.O. Box 116131, Gainesville, Florida 32611

Abstract

We report the detection of luciferase by implementing a bioluminescent assay in microfluidic reactors. The reactors were fabricated in poly(methyl methacrylate) by hot embossing using a mold master with the reactor layouts made by high-precision micromilling. The overall fabrication process was simple to implement and had a quick turnaround time with low cost. Two reactors, one with smooth channels (called reactor I) and the other with staggered herringbone mixers (called reactor II), were studied for the bioluminescent assay. The assay was implemented by introducing a sample and an assay solution into the reactors and then mixing took place to achieve the enzymatic reactions. We found that the mixing efficiency in reactor II was 17.8 times higher than reactor I. Theoretical analysis of the experimental results indicated that the required channel length of mixing was linearly proportional to the flow rate. A calibration curve for luciferase was obtained for both reactors. We found that the detection sensitivity of reactor II was 3 times higher than reactor I. The limit of detection in reactor II was determined to be 0.14 μg/mL luciferase. The device was further exploited to determine the concentration of luciferase samples obtained from in vitro protein expression.

We have recently reported the development of microfluidic devices for protein synthesis, which was realized by transcribing a DNA molecule with a coding sequence into mRNA that was then translated into proteins.[1,2] One of the proteins synthesized in the device was luciferase; we used a microplate reader to detect and verify the production of luciferase. Our goal is to integrate the device with an online detector to measure the amount of protein synthesized. This work represents a step in that direction by developing microfluidic reactors to carry out a bioluminescent reaction to quantify the amount of luciferase.

Luciferase is an enzyme that catalyzes the production of light in the presence of luciferin and adenosine triphosphate (ATP), as indicated by the reaction,[3]

$$\mathrm{ATP+luciferin} \xrightarrow{\text{luciferase}} \mathrm{oxyluciferin+pyrophosphate+AMP+light}$$

This enzymatically catalyzed reaction has been extensively used for bioluminescence detection. Luminescence-based detection approaches are attractive because of their high

* To whom correspondence should be addressed. E-mail: hfan@ufl.edu. Fax: 1-352-392-7303.
[†]Department of Mechanical and Aerospace Engineering, University of Florida.
[‖]Current address: US Genomics, Inc., 12 Gill Street, Suite 4700, Woburn, MA 01801.
[‡]Louisiana State University.
[§]Department of Biomedical Engineering, University of Florida.

SUPPORTING INFORMATION AVAILABLE
Additional information as noted in text. This material is available free of charge via the Internet at http://pubs.acs.org.

sensitivity, wide dynamic range, and relatively simple instrumentation.[3,4] In addition, bioluminescence instrumental setups do not require a light source and the related optics, which are often necessary in other optical approaches. Luciferase-based luminescence detection has also been exploited for microfluidics-enabled microbial sensors,[5] monitoring of dynamic cellular events in cells,[6] quantifying the amount of ATP released from erythrocytes,[7] and analysis of ATP-conjugated metabolites.[8]

To implement the luminescence assay in a microfluidic device, luciferase and the other reagents must be properly mixed to maximize the light production to enhance detection sensitivity. However, effective mixing is difficult to achieve because flows inside a microchannel are laminar due to their low Reynolds number. Molecular diffusion becomes the primary mixing mechanism. As a result, it requires a long channel and takes excessive times to achieve complete mixing. To address this issue, a variety of methods have been reported to generate convective flows for more effective mixing in microfluidic devices. One approach is to exploit external forces to achieve active mixing, including magnetic forces,[9,10] electrokinetic fields,[11–13] ultrasonic forces,[14] and acoustic waves.[15,16] These approaches have been demonstrated to be effective in mixing, but the device fabrication and operation tend to be complicated.

An alternative approach is to use passive mixing without additional energy input. This is often achieved by using irregular channel geometries to stir or laminate fluids to shorten diffusion lengths.[17–24] For example, Locascio's group created a series of slanted wells in a channel and these wells lead to a high degree of lateral transport within the channel with a concomitant rapid mixing of two confluent streams undergoing electroosmotic flow.[18] Whitesides and co-workers used herringbone structures in a channel, creating mixing streams of steady pressure-driven flows at low Reynolds number.[19] Because of no complication in the operation, using the staggered herringbone mixers (SHM) to achieve chaotic advection has become very popular. They have been used in recent years by several research groups for a variety of applications.[19–24]

In this study, we investigated the use of the SHM as a mixing approach to achieve bioluminescence detection of luciferase. First, we employed an alternative process to fabricate the SHM, which was found to be a much simpler approach compared to those reported.[18,19] A brass mold master with device layouts was made by high-precision micromilling; microfluidic devices were then replicated from the mold by hot embossing. The process is simpler and has a quick turnaround time compared to a two-step lithographic process typically used to form herringbone structures in silicon and then to transfer them into a poly (dimethylsiloxane) device,[19] or a process requiring an additional step of laser ablation after microfabrication of microchannels in a plastic device.[18] In addition, manufacturing of low-cost, high-volume plastic parts with microscale features is well-established, evidenced from compact disk (CD) that is injection-molded from plastics. Each blank CD consists of microgrooves and can be manufactured at a cost of less than 40 cents.[25] Second, we studied a reactor with SHM, determined its mixing efficiency, and compared it to a reactor without the SHM. We also examined the required channel length of mixing as a function of the flow rate. Third, we applied the reactors for the bioluminescent detection of luciferase, obtained calibration curves for quantitation, and investigated the detection sensitivity and the limit of detection. In addition, the device was exploited to determine the concentration of luciferase samples obtained from in vitro protein expression.

EXPERIMENTAL SECTION

Reagents and Materials

Poly(methyl methacrylate) (PMMA) sheets (5 mm thick) and cover films (0.5 mm thick) were obtained from Plexiglas MC (GE Polymershapes, New Orleans, LA). QuantiLum recombinant

luciferase and luciferase assay kits were purchased from Promega (Milwakee, WI). Acetylated bovine serum albumin (BSA) was purchased from Sigma-Aldrich (St. Louis, MO) while Alconox detergent was from Fisher Scientific (Atlanta, GA).

Device Fabrication

The layout of the microfluidic reactors is shown in Figure 1a and b. Two reactors referred to as "reactor I" and "reactor II" were used in this work. Each microfluidic reactor was composed of five pairs of inlets, a straight channel connected to a spiral channel, and one outlet. The first pair of inlets and the last pair were used in this work and they are numbered in the figures for easy reference. Reactor II was exactly the same as reactor I except for possessing the SHM in the straight channel. There was one SHM after each pair of inlets; these SHMs are numbered in Figure 1b for easy reference. Each SHM with their corresponding inlets was designed to study the distance of the straight channel needed to achieve mixing. The additional spiral channel would provide sufficient time to complete the reactions when reaction kinetics is slow. Within each SHM, there were five cycles of staggered herringbone ridges. The detail of one cycle of staggered herringbone ridges is illustrated in an exploded view in Figure 1c while its scanning electron micrograph (SEM) is shown in Figure 1d. One cycle consisted of five herringbone ridges with a short section at the top staggered with five herringbone ridges with a short section at the bottom. All straight and spiral channels were 200 μm wide and 100 μm deep, except where specified otherwise. Each herringbone ridge was 50 μm wide and 25 μm high. The length of each side channel connected to an inlet was 4 mm while the straight channel and the spiral channel were 35 and 56 mm long, respectively. The patterns of the devices were designed using AutoCAD and then milled in a 6.3-mm-thick brass plate (353 engravers brass, McMaster-Carr) with a high-precision micromilling machine (Kern MMP 2522). Micromilling was carried out using 500-, 200-, and 50-μm-diameter milling bits at a speed of 40 000 rpm with a feed rate of 200, 120, and 15 mm/min, respectively. The detailed procedures of the micromilling operation have been described previously.[26] Using this micromilled part as a mold, the pattern was hot embossed into PMMA sheets via a hydraulic press (Precision Press TS-21-H-C, City of Industry, CA) with a force of 1000 lb for 4 min at 150 °C. After cleaning with 0.5% Alconox solution and DI water, the PMMA sheet was bonded to a PMMA film at 107 °C for 20 min in a convection oven (4–6 devices were bonded simultaneously in the same oven in one run). Four inlets and one outlet numbered in Figure 1a and b were created by drilling a 400-μm-diameter hole at the end of the corresponding channel after hot embossing. The holes became wells after lamination with the film. Other channel ends without holes were sealed by the thin film since they were not used in this work.

Simulation

Computational simulation of fluid mixing in a microchannel was carried out using commercial computational fluid dynamics (CFD) software, CFD-ACE+ (ESI Group, Huntsville, AL). The width and depth of the channels and ridges were the same as in Figure 1a and b. However, the channel length was shortened to 6 (corresponding to one SHM or five cycles of herringbone ridges) or 1.2 mm (corresponding to one cycle of herringbone ridges) to reduce the computation time. The three-dimensional geometric models of the microchannels were built by CFD-GEOM; the density of mesh elements was studied to produce accurate simulation results. The flow module in CFD-ACE+ solved the incompressible Navier–Stokes equations, assuming a steady and laminar flow of a Newtonian fluid. Two inlets were assigned with a gauge pressure of 10 Pa, filled with fluid 1 or fluid 2 with a diffusion coefficient of 1.0×10^{-6} cm^2/s. No-slip condition was assumed along channel walls, and the outlet was set at atmospheric pressure.

Luminescence Assay

Luciferase is an enzyme that catalyzes luciferin oxidation in the presence of ATP, magnesium ion, and oxygen and generates light with a peak emission at ~560 nm. The commercial luciferase assay kit contains optimal concentrations of luciferin, magnesium, ATP, and other reagents; appropriate reconstitution of these components by following the manufacturer's instructions forms a mixture called luciferase assay reagents (LAR). After LAR is mixed with a sample, the luminescence signal detected indicates the amount of luciferase in the sample. A series of luciferase samples with a concentration from 14.6 ng/mL to 14.6 μg/mL were prepared by diluting a stock solution with cell culture lysis reagent (provided by the luciferase assay kit) and 1 mg/mL BSA. Adding BSA into the mixture prevented proteins from being adsorbed onto the channel walls, eliminating possible background signal.

A luciferase sample was filled in a 50-μL glass syringe (SGE International Pty. Ltd., Austin, TX) and LAR was added into another syringe. Both syringes were installed on a syringe pump (PHD 2000, Harvard Apparatus, Holliston, MA). Each syringe was connected to a fused-silica capillary via a luer-to-microtight assembly (P-662, Upchurch Scientific, Oak Harbor, WA). The capillary was inserted into an inlet of the microfluidic reactor; epoxy glue was applied to the connection to secure the capillary for reagent delivery. The flow rate of the syringe pump was varied to study the effect of the flow rate on the enzymatically catalyzed bioluminescence reactions. Luminescence signals were detected by using a thermoelectrically cooled (−70 °C) CCD camera (Cascade 1K, Roper Scientific, Trenton, NJ) coupled to an optical lens subsystem. The microfluidic device was placed on an X–Y stage that allowed different regions of the device to be imaged. Luminescence images were analyzed using software Winview 32.

RESULTS AND DISCUSSION

Staggered Herringbone Mixers

As mentioned above, SHM were fabricated in plastic microfluidic reactors as shown in Figure 1b. We explored using a high-precision micromilling machine to fabricate a mold master, which was then used for replicating microfluidic devices containing SHM. Replication can be achieved by hot embossing, compression molding, or injection molding while a wide range of thermoplastics may be used. Thousands to millions of plastic devices can be fabricated using one metal mold.[27] The approach of using micromilling (followed by replication) is simple and does not require lithographic processing, producing low cost devices in a short turnaround time.

The micromilling machine used in this work was claimed by the manufacturer to have positional and repetition accuracy of ±1 μm. Our results in Table 1 indicated a difference of a few micrometers in the size of the features from the original design; the relative difference was ~3–4% in the channel width and depth. This difference is acceptable for most microfluidic devices when the feature size is 50–100 μm. Furthermore, significantly smaller differences existed between the feature sizes in the brass mold and the plastic device; the relative difference was ~1% in the channel width and depth. This result suggested a high degree of fidelity during the transfer of the microfeatures from the brass mold to the plastic substrates. The relative difference increased when the channel features became smaller as indicated in the dimension of the ridges in Table 1. Note that the topology of the plastic device was a negative image of the brass mold. In other words, channels in the device corresponded to ridges in the mold. The dimensions of microfeatures were determined by a noncontact profiler (Nanovea ST 400, Allentown, PA).

To study the effects of the SHM on fluid mixing, luciferase was placed in inlet 1 of reactor II, the LAR were placed in inlet 2, and both were simultaneously pumped into the device. When

luciferase meets with the LAR at the T-intersection, catalytical reactions take place and generate luminescence. As a result, the luminescence signal indicates the degree of mixing. Figure 2a shows a top view of luminescence images for reactor II when the flow rate was set at 1 μL/min and the concentration of luciferase was 14.6 μg/mL. These images corresponded to the sections of SHM-1–SHM-5 and the spiral channel of reactor II in Figure 1b. Only a partial section of the SHM was imaged due to the field of view of the camera. These images clearly indicated that luciferase and LAR were completely mixed when they flowed through the SHM. The interfacial line between the two fluids disappeared almost immediately after they entered into the region containing the first SHM. In contrast, in reactor I without the SHM, the two solutions interacted with each other only in the centerline of the entire channel as suggested in Figure 2b. As expected, the two solutions flowed parallel to each other in a laminar profile without any turbulence due to the low Reynolds number. While luciferase diffuses axially into the LAR layer, the thickness of the luminescent trace in the bottom half of the channel increased along the length of the channel. However, this diffusion-based mixing was not complete even at the end of the spiral channel due to the large Peclet number as discussed in the literature.[19]

The mixing efficiency, ε, was analyzed by calculating the luminescence intensity along a line perpendicular to the flow direction by the formula,[28]

$$\varepsilon=\frac{\Delta y\sum_i I_i}{wI_{\max}} \tag{1}$$

where Δy, I_i, w, and $I_{\max}$ represent the interval between sampling points, intensity at sampling point i, width of the channel, and peak intensity when fully mixed, respectively. In other words, ε represents the luminescence intensity at a location along the channel normalized against the maximum intensity. The normalized luminescence intensities at different positions downstream for reactors I and II are plotted in Figure 3. The luminescence intensity in reactor I increased steadily along the microchannel, all the way to the end of the spiral channel (91 mm). In contrast, the luminescence signal in reactor II rapidly intensified, reaching a plateau at 24 mm where SHM-3 was located. The results indicated that the SHM significantly enhanced the efficiency of fluid mixing as reported in the literature.[19]

To compare the results of reactors I and II quantitatively, we followed the treatment developed by Kim et al.[20,21] They showed that the normalized average intensity, ε, is represented by the equation,

$$\varepsilon=1-\exp\left(-\frac{x}{\lambda}\right) \tag{2}$$

where x is the coordinate of the channel downstream (i.e., distance from the merging intersection of the two inlets) and λ is the characteristic length. When x equals λ, ε is equal to 0.632. Therefore, the physical meaning of λ is the required channel length to achieve a mixing efficiency of 63.2%. Using this equation, the experimental data in Figure 3 were plotted, giving the best-fit lines. The resulting λ value of reactor I was 98.0 mm whereas that of reactor II was 5.5 mm. Therefore, the required mixing length to achieve 63.2% mixing efficiency in reactor I was 17.8 times longer than that in reactor II. Because the length of one SHM (five cycles of staggered herringbone ridges) was 6 mm, which is slightly longer than the λ value of reactor II (5.5 mm), we focused on one SHM in the following discussion.

Simulation

To visualize the concentration distribution and the mixing process in channels, we used commercially available CFD software to model reactors I and II. This CFD software has been

used by many others[18,29] to simulate mixing, including SHM.[23] It is well-understood that the smaller the mesh elements, the more accurate the simulation result, but the longer the computation time. We first studied the density of mesh elements required for CFD using a channel of 1.2 mm (the length of one cycle of the staggering herringbone ridges). The dimension of mesh elements was set at 0.833, 1.5625, 3.125, 6.25, and 12.5 μm. We found that the computational residue converged when the dimension of the mesh elements was set at 3.125 μm, indicating an appropriate mesh size. We then studied a channel of 6 cm (the length of one SHM or five cycles of herringbone ridges). The concentration distribution along the channel is shown in Figure 4. The simulation result of reactor I in Figure 4a showed diffusion-based mixing at the interface of the two fluids; the thickness of the interface slowly increased along the channel. This agrees with the result in Figure 2b for a typical laminar flow. In contrast, the simulation result of reactor II in Figure 4b showed a chaotic mixing of two fluids, indicating a helical flow pattern as reported previously.[19,20] This agrees with the result in Figure 2a, in which two fluids mix rapidly along the channel.

Flow Rate

To study the effects of the flow rate on fluid mixing and luminescence reactions, luciferase was introduced into inlet 3 of reactor I or II and LAR was placed in inlet 4. These two fluids were simultaneously pumped into the device and mixed along the channel length. Note that there was only one SHM (SHM-5 in Figure 1b) after inlets 3 and 4. The concentration of luciferase was fixed at 14.6 μg/mL while the flow rate was changed from 1 to 8 μL/min. Figure 5 shows the normalized average intensity as a function of the channel distance for different flow rates. Again, the experimental results were theoretically analyzed using eq 2 and the solid lines represent the best-fit regression curves. The results confirmed that reactor II with the SHM had much higher mixing efficiency compared to reactor I, no matter what the flow rate was. The λ values from the theoretical analysis were 5.8, 7.0, 9.7, and 12.8 mm for reactor II and 77.9, 97.2, 116.8, and 176.4 mm for reactor I, at a flow rate of 1, 2, 4, and 8 μL/min, respectively. We found that the λ value increased linearly as a function of the flow rate as illustrated in Figure 5b.

This linear relationship was true for both reactors. This result can be explained by the fact that the distance along the channel required for mixing was determined by the Péclet number ($Pe = VL/D$, where V is the flow velocity, L is the flow characteristic length such as the channel dimension, and D is the diffusion coefficient).[19] The higher the flow rate (the larger the convective transport), the longer the channel required for mixing.

Luciferase Detection

As discussed in the introduction, one goal of this study was to determine the amount of luciferase synthesized by in vitro protein expression. Luciferase is also frequently used as a reporter gene for measuring promoter activity or transfection efficiency in biological studies. As a result, we studied the detection limit of luciferase and the dynamic range of detection for reactors I and II. A series of concentrations of luciferase were used in the study while the amount of LAR remained the same. Both luciferase and LAR were pumped at a constant flow rate of 1 μL/min. Because the amount of LAR was in excess, the measured luminescence intensity should be proportional to the amount of luciferase. A calibration curve between the intensity and the luciferase concentration was obtained (see the figure in Supporting Information). The correlation coefficient of the best-fit linear regression line was 0.9944. The luminescence intensity was measured in the region of the spiral channel where mixing and reactions should be completed in reactor II. Three repeat experiments were performed for each data point; the standard deviations are indicated by the error bars. The results showed a dynamic detection range of more than 2 orders of magnitude (from 0.1 to 15 μg/mL). The detection sensitivity was 3.0 times higher in reactor II than reactor I because of more efficient mixing

by the SHM. The detection limit of luciferase in reactor II was determined to be 0.14 μg/mL by defining an analytical signal equal to three times the standard deviation of the blank sample.

After establishing the calibration curve, we used reactor II to determine the concentration of luciferase synthesized using in vitro protein expression. The protein expression was carried out using a wheat germ expression kit in a microcentrifuge tube as reported previously.[1,2] The synthesized luciferase and LAR were pumped into inlets 3 and 4 of reactor II at a flow rate of 1 μL/min. The image of the luminescence signal is shown in the inset of the figure in Supporting Information. Note that we did not see signal when the experiment was implemented in reactor I due to the higher detection limit. Based on the calibration curve, the concentration of the synthesized luciferase in this experiment was determined to be 0.15 ng/μL. With the protein expression in the device >10 times higher than in a microcentrifuge tube,[1,2] the result suggested that it was feasible to detect the expression products produced in an integrated device.

CONCLUSIONS

We reported the use of high-precision micromilling to make a mold master, which was then exploited to fabricate PMMA microfluidic devices using hot embossing. This approach is simpler than those involving photolithography, has a quick turnaround time in terms of device production, and the cost of producing devices is low. The method is especially beneficial for rapidly producing prototypes as well as for device topology optimization and provides flexibility in the choice of substrate materials.

We confirmed other reports that the SHM is an effective mixer configuration. We developed a microfluidic reactor consisting of the SHM to implement luminescence detection of luciferase. We found that the mixing efficiency of reactor II (with the SHM) was 17.8 times better than reactor I (without the SHM). Our theoretical analysis of the experimental results suggested that the required channel length to achieve mixing was linearly proportional to the flow rate.

We also employed reactor II to determine the concentration of luciferase samples obtained from in vitro protein expression. As we demonstrated previously,[1,2] luciferase can be synthesized in a microfluidic device. These results suggested that it is feasible to integrate the components for luciferase synthesis with an online detector.

Acknowledgements

This work is supported in part by the Research Opportunity Incentive Seed Fund from the University of Florida, and the grant from Defense Advanced Research Projects Agency (DARPA) via Micro/Nano Fluidics Fundamentals Focus Center at the University of California at Irvine. We thank Mr. Jason Guy at Louisiana State University for micromilling the mold master.

References

1. Mei Q, Fredrickson CK, Simon A, Khnouf R, Fan ZH. Biotechnol Prog 2007;23:1305–1311. [PubMed: 17924644]
2. Mei Q, Fredrickson CK, Lian W, Jin S, Fan ZH. Anal Chem 2006;78:7659–7664. [PubMed: 17105156]
3. Kricka LJ. Anal Biochem 1988;175:14–21. [PubMed: 3072882]
4. Roda A, Pasini P, Mirasoli M, Michelini E, Guardigli M. Trends Biotechnol 2004;22:295–303. [PubMed: 15158059]
5. Tani H, Maehana K, Kamidate T. Anal Chem 2004;76:6693–6697. [PubMed: 15538793]
6. Davidsson R, Boketoft A, Bristulf J, Kotarsky K, Olde B, Owman C, Bengtsson M, Laurell T, Emneus J. Anal Chem 2004;76:4715–4720. [PubMed: 15307781]
7. Price AK, Fischer DJ, Martin RS, Spence DM. Anal Chem 2004;76:4849–4855. [PubMed: 15307797]

8. Liu BF, Ozaki M, Hisamoto H, Luo Q, Utsumi Y, Hattori T, Terabe S. Anal Chem 2005;77:573–578. [PubMed: 15649055]
9. Lu LH, Ryu KS, Liu C. J Microelectromech Syst 2002;11:462–469.
10. Lemoff AV, Lee AP. Biomed Microdevices 2003;5:55–60.
11. Oddy MH, Santiago JG, Mikkelsen JC. Anal Chem 2001;73:5822–5832. [PubMed: 11791550]
12. Wu HY, Liu CH. Sens Actuators, A 2005;118:107–115.
13. Glasgow I, Batton J, Aubry N. Lab Chip 2004;4:558–562. [PubMed: 15570365]
14. Yang Z, Matsumoto S, Goto H, Matsumoto M, Maeda R. Sens Actuators, A 2001;93:266–272.
15. Liu RH, Lenigk R, Grodzinski P. J Microlithogr, Microfabr Microsyst 2003;2:178–184.
16. Yaralioglu GG, Wygant IO, Marentis TC, Khuri-Yakub BT. Anal Chem 2004;76:3694–3698. [PubMed: 15228343]
17. Liu RH, Stremler MA, Sharp KV, Olsen MG, Santiago JG, Adrian RJ, Aref H, Beebe DJ. J Microelectromech Syst 2000;9:190–197.
18. Johnson TJ, Ross D, Locascio LE. Anal Chem 2002;74:45–51. [PubMed: 11795815]
19. Stroock AD, Dertinger SKW, Ajdari A, Mezic I, Stone HA, Whitesides GM. Science 2002;295:647–651. [PubMed: 11809963]
20. Kim DS, Lee SW, Kwon TH, Lee SS. J Micromech Microeng 2004;14:798–805.
21. Kim DS, Lee SH, Kwon TH, Ahn CH. Lab Chip 2005;5:739–747. [PubMed: 15970967]
22. Howell PB, Mott DR, Fertig S, Kaplan CR, Golden JP, Oran ES, Ligler FS. Lab Chip 2005;5:524–530. [PubMed: 15856089]
23. Yang JT, Huang KJ, Lin YC. Lab Chip 2005;5:1140–1147. [PubMed: 16175271]
24. Lynn NS, Dandy DS. Lab Chip 2007;7:580–587. [PubMed: 17476376]
25. Fredrickson CK, Xia Z, Das C, Ferguson R, Tavares FT, Fan ZH. J Microelectromech Syst 2006;15:1060–1068.
26. Hupert ML, Guy WJ, Llopis SD, Shadpour H, Rani S, Nikitopoulos DE, Soper SA. Microfluidics Nanofluidics 2007;3:1–11.
27. Boone TD, Fan ZH, Hooper HH, Ricco AJ, Tan H, Williams SJ. Anal Chem 2002;74:78A–86A.
28. Hosokawa K, Fujii T, Nojima T, Shoji S, Yotsumoto A, Endo I. J Micromechatronics 2000;1:85–98.
29. Devasenathipathy S, Santiago JG, Wereley ST, Meinhart CD, Takehara K. Exp Fluids 2003;34:504–514.

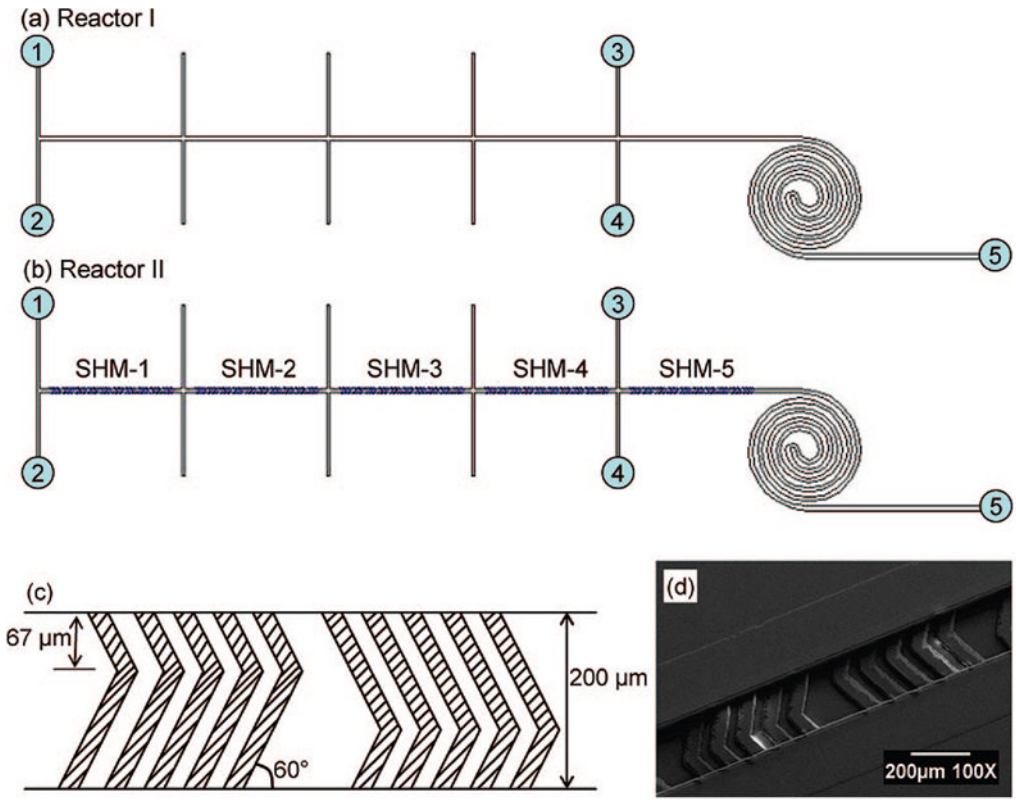

Figure 1.

(a) Schematic diagram of a microfluidic device referred to as reactor I. The device consisted of multiple T-shaped inlets, a straight channel, a spiral channel for reactions, and one outlet. The inlets used in this work were numbered. (b) Schematic diagram of reactor II. It is the same as reactor I except for the SHM included in the straight channel region. (c) The architectural details of one cycle of the staggered herringbone ridges. (d) SEM photograph of the SHM on the bottom surface of a PMMA device.

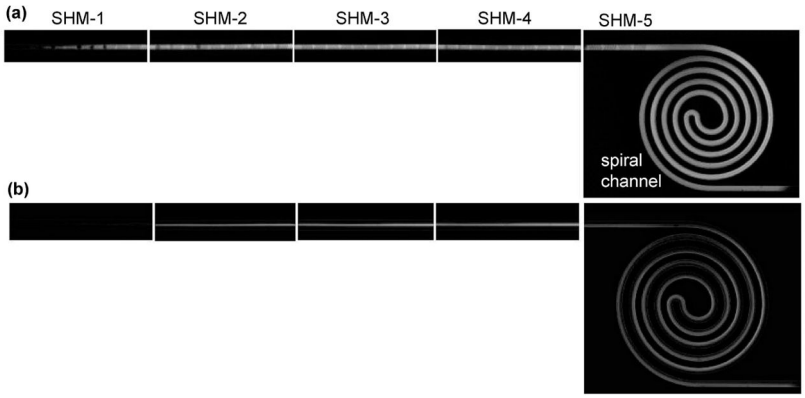

Figure 2.
Luminescence images of microchannels indicating luminescence reactions between luciferase and luciferase assay reagents. Luminescence in the entire channel of reactor II (a) indicated complete mixing whereas luminescence signal present only in the bottom half of the channel in reactor I (b) suggested partial mixing between luciferase and LAR.

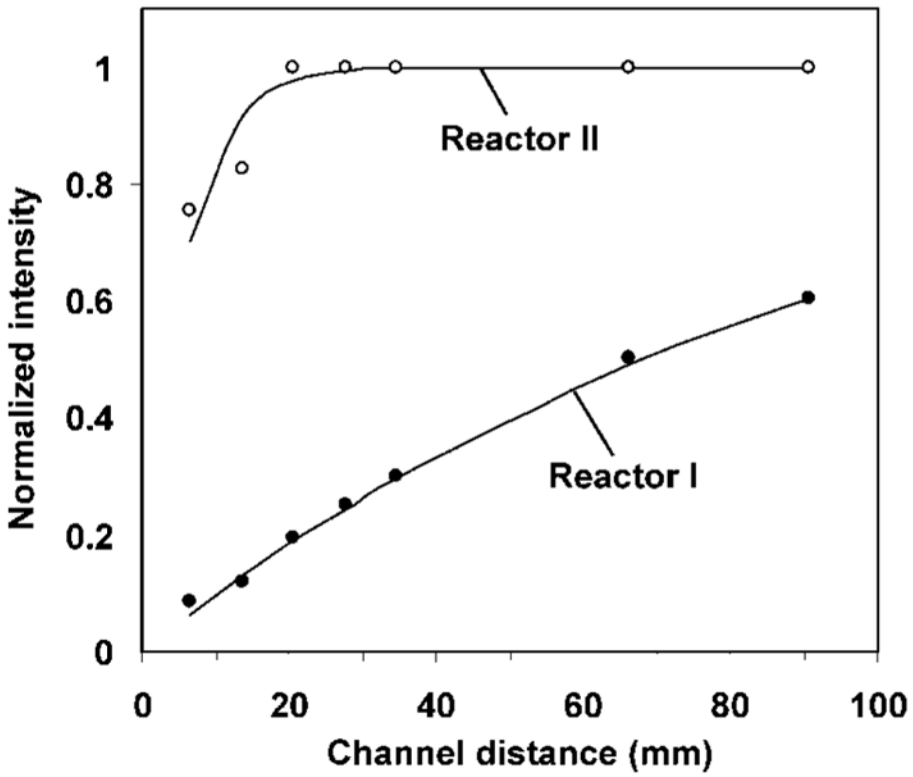

Figure 3.
Normalized luminescence intensity along the length of the mixing channel using reactor I (without mixers) and reactor II (with the SHM). The flow rate was 1 μL/min. The solid lines represent theoretical analysis discussed in the text and were fit to the experimental data.

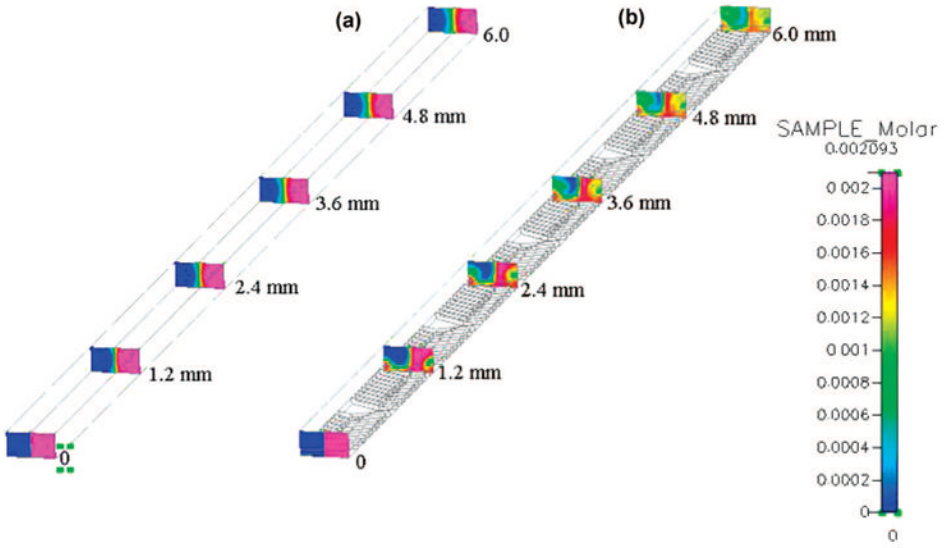

Figure 4.
Concentration distribution of two fluids in cross sections along the mixing channel in (a) reactor I and (b) reactor II. The flow rate was 1 μL/min.

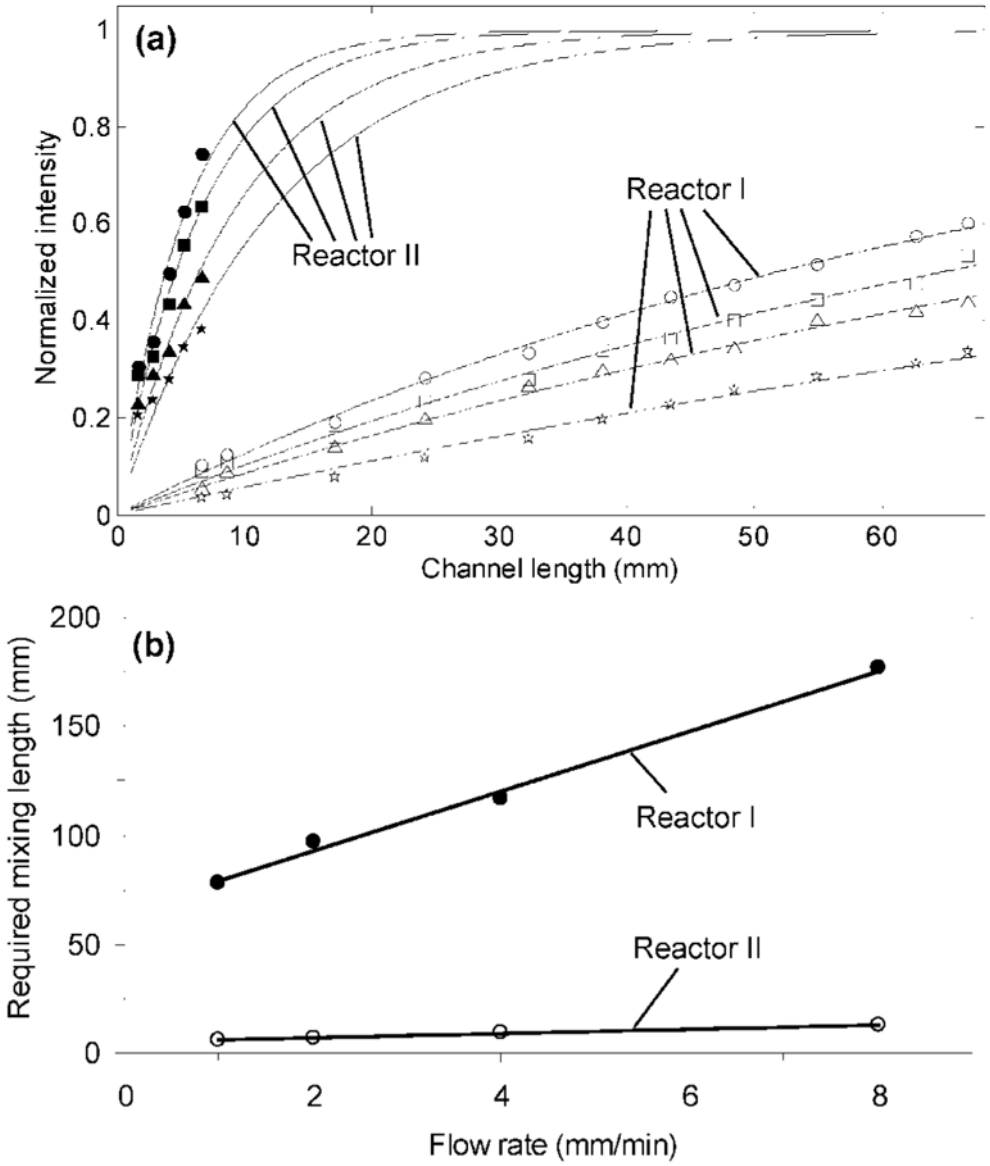

Figure 5.

(a) Effects of the flow rate on the relationship between the luminescent intensity and the channel distance in reactor I and reactor II. The flow rates of samples and reagents were 1 (circles), 2 (squares), 4 (triangles), and 8 μL/min (stars), respectively. The solid lines represent theoretical analysis discussed in the text and were fit to the experimental data. (b) Plot of the required mixing length (the λ values) as a function of the flow rate.

Table 1

Dimensions of Channels and Other Microfeatures in the Original Design, the Brass Mold, and the Embossed Plastic Microfluidic Devices

	original design (μm)	mold master (μm)	relative difference (%)	embossed device (μm)	relative difference (%)
channel width	200	208.3 ± 0.6	4.2	205.3 ± 1.5	1.4
channel depth	100	96.7 ± 0.5	3.3	95.7 ± 1.5	1.0
ridge height	25	23.3 ± 0.2	6.8	22.8 ± 0.2	2.1